



Kinematic Changes in a Mouse Model of Penetrating Hippocampal Injury and Their Recovery After Intranasal Administration of Endometrial Mesenchymal Stem Cell-Derived Extracellular Vesicles

OPEN ACCESS

Edited by:

Vicente Herranz-Pérez,
University of Valencia, Spain

Reviewed by:

Fernando Ezquer,
Universidad del Desarrollo, Chile
Zheng Zachory Wei,
Emory University, United States

*Correspondence:

Sergio Horacio Dueñas-Jiménez
sduenas@cucs.udg.mx

Specialty section:

This article was submitted to
Cellular Neuropathology,
a section of the journal
Frontiers in Cellular Neuroscience

Received: 01 July 2020

Accepted: 14 August 2020

Published: 10 September 2020

Citation:

León-Moreno LC,
Castañeda-Arellano R,
Aguilar-García IG,
Desentis-Desentis MF,
Torres-Anguiano E,
Gutiérrez-Almeida CE,
Najar-Acosta LJ, Mendizabal-Ruiz G,
Ascencio-Piña CR,
Dueñas-Jiménez JM,
Rivas-Carrillo JD and
Dueñas-Jiménez SH
(2020) Kinematic Changes in a
Mouse Model of Penetrating
Hippocampal Injury and Their
Recovery After Intranasal
Administration of Endometrial
Mesenchymal Stem Cell-Derived
Extracellular Vesicles.
Front. Cell. Neurosci. 14:579162.
doi: 10.3389/fncel.2020.579162

Lilia Carolina León-Moreno^{1,2}, Rolando Castañeda-Arellano³,
Irene Guadalupe Aguilar-García¹, María Fernanda Desentis-Desentis²,
Elizabeth Torres-Anguiano², Coral Estefanía Gutiérrez-Almeida¹,
Luis Jesús Najar-Acosta², Gerardo Mendizabal-Ruiz⁴, César Rodolfo Ascencio-Piña⁴,
Judith Marcela Dueñas-Jiménez¹, Jorge David Rivas-Carrillo² and
Sergio Horacio Dueñas-Jiménez^{1*}

¹Laboratory of Neurophysiology, Department of Neuroscience, University Center for Health Sciences, University of Guadalajara, Guadalajara, Mexico, ²Department of Biomedical Sciences, University Center of Tonalá, University of Guadalajara, Guadalajara, Mexico, ³Laboratory of Tissue Engineering and Transplant, Department of Physiology, cGMP Cell Processing Facility, University Center for Health Sciences, University of Guadalajara, Guadalajara, Mexico, ⁴Department of Computer Sciences, University Center of Exact Sciences and Engineering, University of Guadalajara, Guadalajara, Mexico

Locomotion speed changes appear following hippocampal injury. We used a hippocampal penetrating brain injury mouse model to analyze other kinematic changes. We found a significant decrease in locomotion speed in both open-field and tunnel walk tests. We described a new quantitative method that allows us to analyze and compare the displacement curves between mice steps. In the tunnel walk, we marked mice with indelible ink on the knee, ankle, and metatarsus of the left and right hindlimbs to evaluate both in every step. Animals with hippocampal damage exhibit slower locomotion speed in both hindlimbs. In contrast, in the cortical injured group, we observed significant speed decrease only in the right hindlimb. We found changes in the displacement patterns after hippocampal injury. Mesenchymal stem cell-derived extracellular vesicles had been used for the treatment of several diseases in animal models. Here, we evaluated the effects of intranasal administration of endometrial mesenchymal stem cell-derived extracellular vesicles on the outcome after the hippocampal injury. We report the presence of vascular endothelial growth factor, granulocyte-macrophage colony-stimulating factor, and interleukin 6 in these vesicles. We observed locomotion speed and displacement pattern preservation in mice after vesicle treatment. These mice had lower pyknotic cells

Abbreviations: DLS, Dynamic Light Scattering; DPI, Days Post-Injury; eMSC, Endometrial Mesenchymal Stem Cells; eMSC-EVs, Endometrial Mesenchymal Stem Cells derived Extracellular Vesicles; EVs, Extracellular Vesicles; IN, Intranasal; MSCs, Mesenchymal Stem Cells; mNSS, Modified Neurological Severity Score; TBI, Traumatic Brain Injury; TEM, Transmission Electron Microscopy.

percentage and a smaller damaged area in comparison with the nontreated group, probably due to angiogenesis, wound repair, and inflammation decrease. Our results build up on the evidence of the hippocampal role in walk control and suggest that the extracellular vesicles could confer neuroprotection to the damaged hippocampus.

Keywords: kinematic analysis, extracellular vesicles, endometrial mesenchymal stem cells, penetrating hippocampal injury, neuronal preservation

INTRODUCTION

Hippocampus is a susceptible brain structure to neurodegenerative diseases (Nikonenko et al., 2009), mainly related to memory, learning, and spatial orientation (Andersen et al., 2007). However, it is related to the sensory-motor system in murine models (Bland, 2009; López Ruiz et al., 2015; Bland et al., 2016), and its role in the gait control has been well known (Beauchet et al., 2019). Speed changes due to neuron loss in dorsal rat hippocampus and the interruption of the sensory-motor circuitry are described (López Ruiz et al., 2015). Lesions or degeneration in this structure impairs a variety of motor and behavioral tasks in mice (Cernak et al., 2014; Tucker et al., 2017; Hwang et al., 2018; Khan et al., 2018), including speed locomotion changes. Coordination between the hippocampus and lateral septum occurs through theta oscillations and facilitates theta inputs to the lateral hypothalamus, which in turn controls speed locomotion (Bender et al., 2015). Nucleus incertus stimulation augments theta power in the hippocampus and accelerates locomotion speed. This is mediated, in part, through the medial septum nucleus pathway to the hippocampus (Lu et al., 2020). However, less is known about locomotion kinematics disruption after hippocampal injury in mice, mainly because of the lack of a methodology useful to analyze the data. Our first aim was to study kinematic changes in a mouse model of penetrating hippocampal injury with our new developed methodology. To date, there is no model that affects hippocampus without damage of the cortex. This model reflects hippocampal injury caused by mild to moderate traumatic brain injury (TBI) in the hippocampus. TBI could affect connectivity of hippocampus (Girgis et al., 2016; Yan et al., 2016) probably due to cellular and synaptic loss secondary to the trauma (Atkins, 2011). Neurodegenerative pathologies and dementia could develop after TBI (Shively et al., 2012). Gait variability has been described for normal aging and patients with mild cognitive impairment, dementia, or Alzheimer disease (Montero-Odasso et al., 2009; Papp et al., 2014; O'Shea et al., 2016; Beauchet et al., 2019). To date, there is no effective treatment for TBI or any of the subsequent pathologies. Currently, mesenchymal stem cells (MSCs) are widely used in both research and cell-based therapy for various human diseases, including neurological and neurodegenerative disorders (Jeong et al., 2014; Gómez-Virgilio et al., 2018). Human endometrium has been reported as an attractive and accessible source for MSCs (Meng et al., 2007; Musina et al., 2008; Gargett et al., 2009). Endometrial MSCs (eMSCs) can be obtained without invasive procedures (Du et al., 2016) and possess a higher proliferation rate and migration capacity compared with MSCs obtained from other sources

(Alcayaga-Miranda et al., 2015; Du et al., 2016). These cells can be differentiated into several lineages, including neurons (Meng et al., 2007). In this study, we use eMSCs to expand the knowledge of its effects on brain injuries. MSCs secrete both growth and anti-inflammatory factors through the secretion of extracellular vesicles (EVs; Drago et al., 2013; Kupcova Skalnikova, 2013). The EVs derived from MSCs (EV-MSCs) are round, and small vesicles originated from endosomes that are membrane-bound. EVs contain regenerative and neuroprotective molecules (Lötvall et al., 2014; Pachler et al., 2017), which could induce angiogenesis and neurovascular plasticity and improve neurobehavioral performance (Doepfner et al., 2015; Paquet et al., 2015; Chen et al., 2016; Kim et al., 2016; Zhang et al., 2017; Williams et al., 2019). Furthermore, intranasal (IN) administration route allows MSC-EVs to reach the brain directly. After 24 h of IN administration, EVs had been found in the cell cytoplasm of neurons, glia and endothelium in the olfactory bulb, cerebral cortex, dorsal and ventral striatum, thalamus, hypothalamus, brainstem, basal forebrain, and dorsal hippocampus (Long et al., 2017; Ezquer et al., 2019), grouped inside the cytoplasm of dentate hilar, CA3, and CA1 pyramidal and dentate granule neurons and nearby astrocyte and microglial processes (Long et al., 2017). In animal models, eMSC-derived EVs (eMSC-EVs) proved to be efficient for the treatment of hepatic failure (Chen et al., 2017), cardioprotection (Wang et al., 2017), diabetic wound healing (Dalirfardouei et al., 2019), Asherman syndrome (Saribas et al., 2019), and type 1 diabetes (Mahdipour et al., 2019). Further investigation is required to determine the role of eMSC-EVs in neuroprotection from direct damage in mouse brain tissue.

We show speed reduction and metatarsus kinematics changes after the hippocampal lesion. Further, behavioral outcomes improvements, restoration of locomotion speed and metatarsus kinematics, the decrease of pyknotic cells, and lesion area reduction were also observed after eMSC-EV treatment.

MATERIALS AND METHODS

All materials described below are available upon request to any interested researchers.

Animals

Animal use and protocols were approved by the “Comité Institucional de Cuidado y Uso de Animales de Laboratorio (CICUAL),” affiliated to the University of Guadalajara and endorsed to “Comisión Nacional de Bioética” (CONBIOÉTICA-14-CEI-002-20191003). All animals were treated following the Mexican Official Norm guidelines (NOM-062-ZOO-1999) and

the National Institutes of Health Guide Publication No. 8023 (revised in 1996) for the Care and Use of Laboratory Animals. Adult male C57BL6 mice (20–25 g of weight) were used. We put the animals in groups of five, in plastic cages with a 12-h light–dark cycle at room temperature ($22^{\circ}\text{C} \pm 2^{\circ}\text{C}$) and constant humidity. Water and food were available *ad libitum*. We used a minimal number of animals and minimized their suffering to obtain reliable results.

Experimental Study Groups

We divided mice into three groups of five animals each: cortex-injured group (CI), hippocampus-injured without treatment group (HI), and hippocampus-injured with EV treatment group (HIEV). After surgery, we randomly divided hippocampus-injured mice into nontreated and treated groups. We used the CI group to determine the effect of sensorimotor cortex damage caused by penetrating injury. We performed kinematic and open-field (OF) locomotion analyses in the same animals. We made a histological analysis on these subjects, immediately after the last kinematic assay (7 days after the penetrating injury). We administered eMSC–EVs intranasally on Day 1 after injury in a dose of 500 μg of EV protein per kg of animal weight.

Brain Injury Model

We used isoflurane gas at 5% for induction and 2–3% for anesthesia and performed surgeries under aseptic conditions. After verifying the absence of pain reflexes, we placed mice in a stereotaxic frame, and a head incision over the middle line was made. A cleft was drilled into the left parietal bone to expose the meninges, and a 0.5-mm-diameter sterile steel cannula was placed horizontally 1.2 and 2.5 mm behind Bregma, according to Paxinos and Franklin coordinates. We lowered a cannula to a 2-mm depth for the hippocampus-injured groups and to 1 mm in the cortex-injured group, displaced rostrally 1 mm (-1.5 from Bregma), and pulled out. We applied pressure over the injury to stop the bleeding. After the procedure, we sutured the scalp incision with 4–0 nylon sutures using lidocaine at 2%. After the surgery, we placed mice in a heat blanket for 30 min. Then, mice received antibiotics for 3 days (Enroxil 2 mg/kg) and analgesics (meloxicam 2 mg/kg).

MSC Culture and Characterization

As xenograft tissue models had been successfully used, we isolated eMSCs from one adult human donor with written informed consent. These cells were provided by CryoVida, Banco de Células Madre Humanas, a stem cell bank certified and approved by COFEPRIS (license no. 18-TR-14-039-0002). Passage 2 cells were thawed at 37°C , washed with Hanks balanced salt solution (Sigma–Aldrich), and plated directly at a concentration of 7×10^6 cells/ 75 cm^2 in tissue culture flasks (Corning) with a xeno-free medium. All cells were cultured at 37°C in an incubator with 5% CO_2 . After cell confluence, the cells were continuously expanded under the same conditions, replacing the medium every 2–3 days. We used only cells in passages three to six and employed Accutase (Sigma–Aldrich) for cell passage. To evaluate the characteristics of the eMSC by flow cytometry, we determined the presence of surface MSC markers CD105, CD73, and CD90 and the absence of hematopoietic

markers CD45 and CD34. The MSCs are sterile [negative for bacteria, yeast, fungi, mycoplasma (<10 colony-forming units), and endotoxin ($<5 \text{ EU/kg/h}$)].

Extracellular Vesicle Obtention and Characterization

For conditioned media obtention, we removed the xeno-free medium, and the cell layer washed with Hanks solution. We replaced the media for a protein-free solution and incubated the culture at 37°C and 5% of CO_2 . We recovered the medium at 48 h and was either stored at -80°C or used directly to isolate EVs. EVs were isolated from the cell culture media *via* multistep centrifugation at 4°C and ultrafiltration. We centrifuged cell culture media at 300 g for 3 min, and the supernatant was removed and centrifuged at 2,000 g for 10 min to remove small debris. The resulting media were further centrifuged at 10,000 g for 30 min. The supernatant is removed and placed in an Amicon Ultra-15 tube (30-kDa cutoff, Merck Millipore) and centrifuged at 5,000 g for 20 min. The obtained EVs were maintained at -80°C for further analysis.

We characterized the EVs from three independent experiments. We quantified EVs by measuring the total protein concentration using the micro-bicinchoninic acid protocol (Thermo Fisher Scientific) and analyzing particle size using dynamic light scattering (DLS) in a Zetasizer NANO ZS90 analyzer (Malvern), according to manufacturer's instructions. The morphology of the EVs was assessed by transmission electron microscopy (TEM). We evaluated the characteristics of the isolated vesicles with the extraction of equal amounts of protein for Western blotting to detect the expression of Tsg101 (Santa Cruz Biotechnology).

We determine the presence of proinflammatory and anti-inflammatory cytokines of our interest: interleukin 17A (IL-17A), IL-17F, IL-23, IL-10, IL-6, IL-1 β , tumor necrosis factor α (TNF- α), interferon γ (IFN- γ), and the following growth factors: granulocyte–macrophage colony-stimulating factor (GM-CSF) and vascular endothelial growth factor (VEGF) using the MILLIPLEX Multi-Analyte Profiling (MAP) Human Cytokine/Chemokine Kit (catalog no. HCYTOMAG-60K) and Human TH17 (catalog no. HTH17MAG-14K), run on a Luminex platform, according to manufacturer's recommendations (Merck Millipore). For quality assurance, each sample was run twice, and the mean derived for each sample, using it as the index value. Kit-supplied quality controls and standards were run on each plate in duplicate and confirmed to fall within the expected range. Where an analyte level was below detection limits, we reported it as the lowest standard value. We analyzed the obtained fluorescence data with Beadview software.

IN Administration of Extracellular Vesicles

We performed the procedure of IN administration as described elsewhere (Long et al., 2017; Ezquer et al., 2019), with minimal modifications. Briefly, anesthetized animals were placed in a supine position, and the ventral surface of the head and neck is maintained horizontal. We administered the eMSC–EV preparations *via* the olfactory pathway using a 10- μl Hamilton

microsyringe, in aliquots of 5 μ l, and alternating nostrils. We waited for 2 min between each administration. Each mouse received a total of 500 μ g of EVs (released by 5×10^6 eMSCs) protein per kilogram of animal weight diluted in 25 μ l of EV preparation 24 h after the penetrating brain injury [1 day postinjury (DPI)] as described before for TBI and stroke animal models (Xin et al., 2013; Zhang et al., 2015, 2017).

Neurological Outcome and Open-Field Tests

We used a modified Neurological Severity Score (mNSS) by a blinded investigator to determine the balance ability, motor functions, and sensory reflexes in mice as described before (Singh et al., 2018), with slight modifications: the prehensile test was incorporated to the 15-point scale (0–3 points), resulting in an 18-point scale in this study. We assigned a score of 0 to animals with normal behavior, and 18 is the score of the most severe neurological outcome. We tested mice before the injury (Day 0) and in days 1, 3, 5, and 7 postinjury.

We evaluated locomotor activity as well as anxiety, in an OF test before and 7 DPI. We used mice recorded before the injury (Day 0) as control for further comparisons. The OF arena was made of a wooden square box (32 \times 45 cm) with a 30-cm-high wall. The floor is divided into 16 quadrants (11.25 \times 8 cm) and subdivided into two imaginary squares called center and periphery. We consider the 12 quadrants adjacent to the walls as periphery. We individually placed mice in the center of the open field and allowed to explore the box for 10 min, cleaning the box using 70% ethanol and water after each mouse evaluation. We recorded mice using a Nikon camera with a resolution of 30 fps and analyzed them with the ImageJ software. We also determined the seconds the animal spent in the periphery of the open field. We analyzed the total distance traveled (cm) by mice and calculate the locomotion speed (cm/s). In all cases, we eliminated the time when mice remained still.

Tunnel Walk Recordings

We obtained kinematic records before (Day 0) and after 7 DPI. We took mice recorded before the injury as a control group for further comparisons. We took video recordings of the animals while walking on a transparent Plexiglas tunnel (tunnel walk), using two synchronized cameras that record left and right hindlimbs simultaneously. We set the cameras to record at 240 fps with a resolution of 1,280 \times 720 pixels. Postprocessing was applied to the resulting videos to remove distortion due to the lenses by estimation of homography matrix using four points on the image (Ascencio-Piña et al., 2020). We separate the steps of interest using the manual definition of instants corresponding to the beginning and end of the step. Manual annotation of the points of interest: knee, ankle, and metatarsus, was performed on each frame of the video for each step using a custom-made software, called “ratwalk” to obtain the coordinates (x, y) of each point. These values were introduced into a software developed in our laboratory to assess the locomotion speed and kinematics analyses. Each of the steps of the mice captured on the video was analyzed separately.

Step Classification

We selected and analyzed five to seven steps in the left and right hindlimbs in each mouse. Because of the diversity of steps observed between and within groups, we evaluated the distribution of types of steps for each group before and after the injury. We classified them into Type A: the step was equal in time in both hindlimbs. Type B steps were those in which the mice took shorter steps with both hindlimbs, whereas Type C were the steps in which left hindlimb stride was longer than the right stride, and Type D steps were the opposite: right hindlimb stride was longer than the left one.

Locomotion Speed Analysis

We determined the speed of the step (left and right) using software developed in our laboratory, which allows us to evaluate treatment effectiveness. A control group was defined using the measurements of all the steps of all mice before the injury. Each of the steps of the mice was analyzed separately. For each step, the length and speed of the step were calculated using the x coordinates (horizontal axis) of the metatarsus. We analyzed the step speed statistics of all the groups with and without considering the kind of steps and performed statistical hypothesis tests to evaluate the differences in the distributions of the groups.

Displacement Analysis

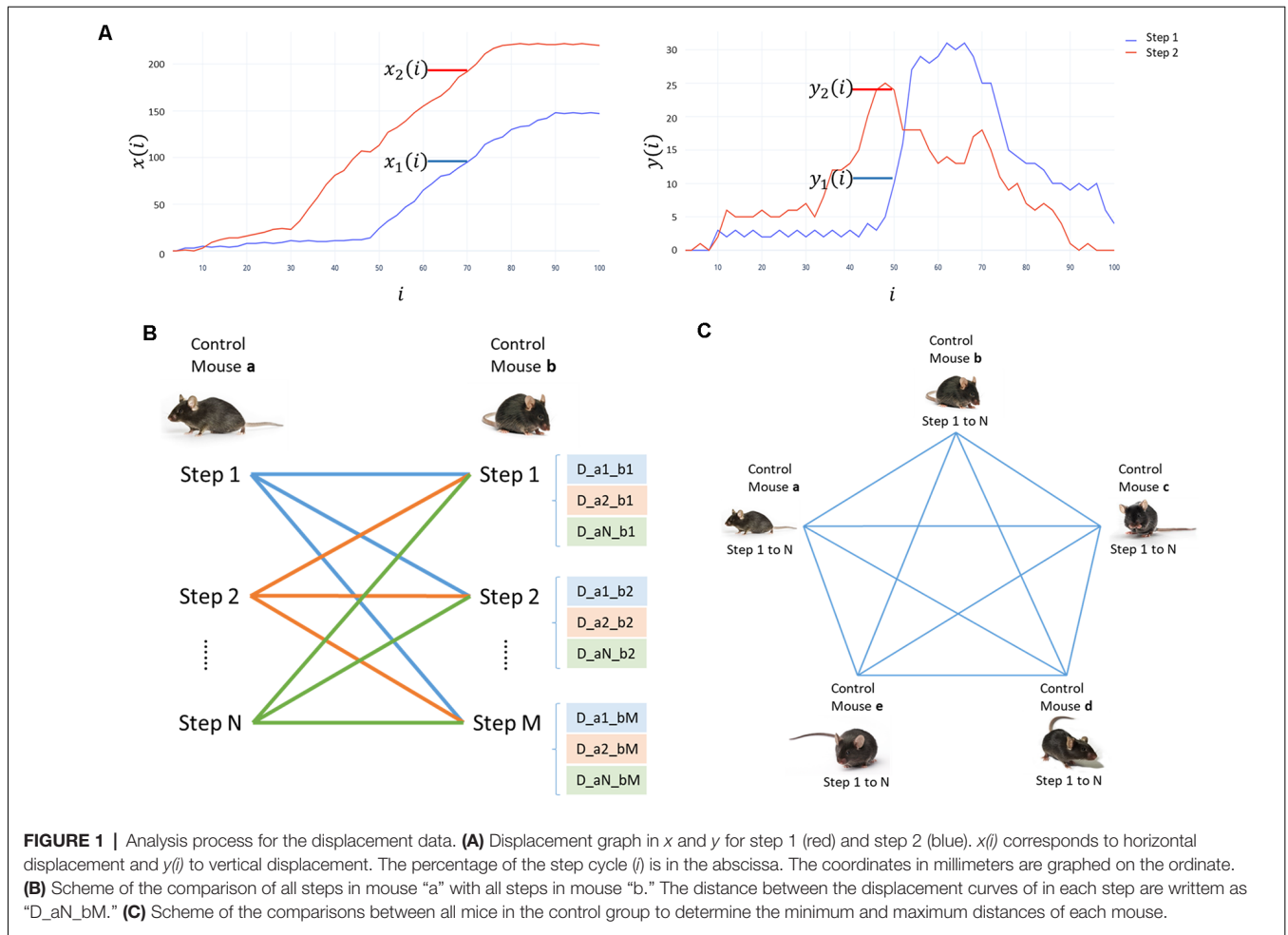
To assess locomotion kinematics pattern analysis, we generated displacement curves on the horizontal and vertical axes with respect to time for each point of interest described before. All curves were normalized with respect to the step using a value range from 1 to 100 employing a spline-based interpolation.

To determine the kinematic changes between groups, we compared the displacement curves among all studied mice. The difference between the curves was calculated using the Euclidean distance between each of the points of the normalized curve on the horizontal (x) and vertical (y) directions as follows:

$$D_{<1,2>} = \frac{1}{200} \sqrt{\sum_{i=1}^{100} (x_1(i) - x_2(i))^2 + \sum_{i=1}^{100} (y_1(i) - y_2(i))^2}$$

where $D_{<1,2>}$ is the squared error between every point of the normalized curves, defined as distance (D); “ $x_1(i) - x_2(i)$ ” is the difference (d) between the coordinates in x , and “ $y_1(i) - y_2(i)$ ” in y of every point in the graph, when comparing two steps (1 and 2; **Figure 1A**); and “ i ” is the percent in the step cycle.

We compared all the curves of every mouse in the control group. Every step curve of a mouse (a) was compared to the curves of a different control mouse (b; **Figure 1B**), and sequentially with each displacement curve of all mice in the control group (**Figure 1C**). For each mouse, we selected two pairs of curves: the most similar ones to calculate the minimum distance (D_{Min}); and the most divergent ones to calculate the maximum distance (D_{Max}). These values indicate the minimum and maximum distances between the steps in control. We used those as a reference of the expected results and to contrast them with the distances obtained when comparing mice in other groups with controls.



We compared every step curve of the mice in CI, HI, and HIEV with each displacement curve of mice in the control group and selected the two pairs of curves mentioned before per mouse. Thus, we calculated the minimum (D_{Min}) and maximum (D_{Max}) differences for every mouse when comparing with a control mouse. D_{Min} values comparison will demonstrate the differences observed when we contrast the most alike curves in all groups, whereas D_{Max} values analysis described the differences in the curves that are already different between each other. We graphed these values in a box plot and performed statistical hypothesis tests to evaluate the differences in the distributions of the groups.

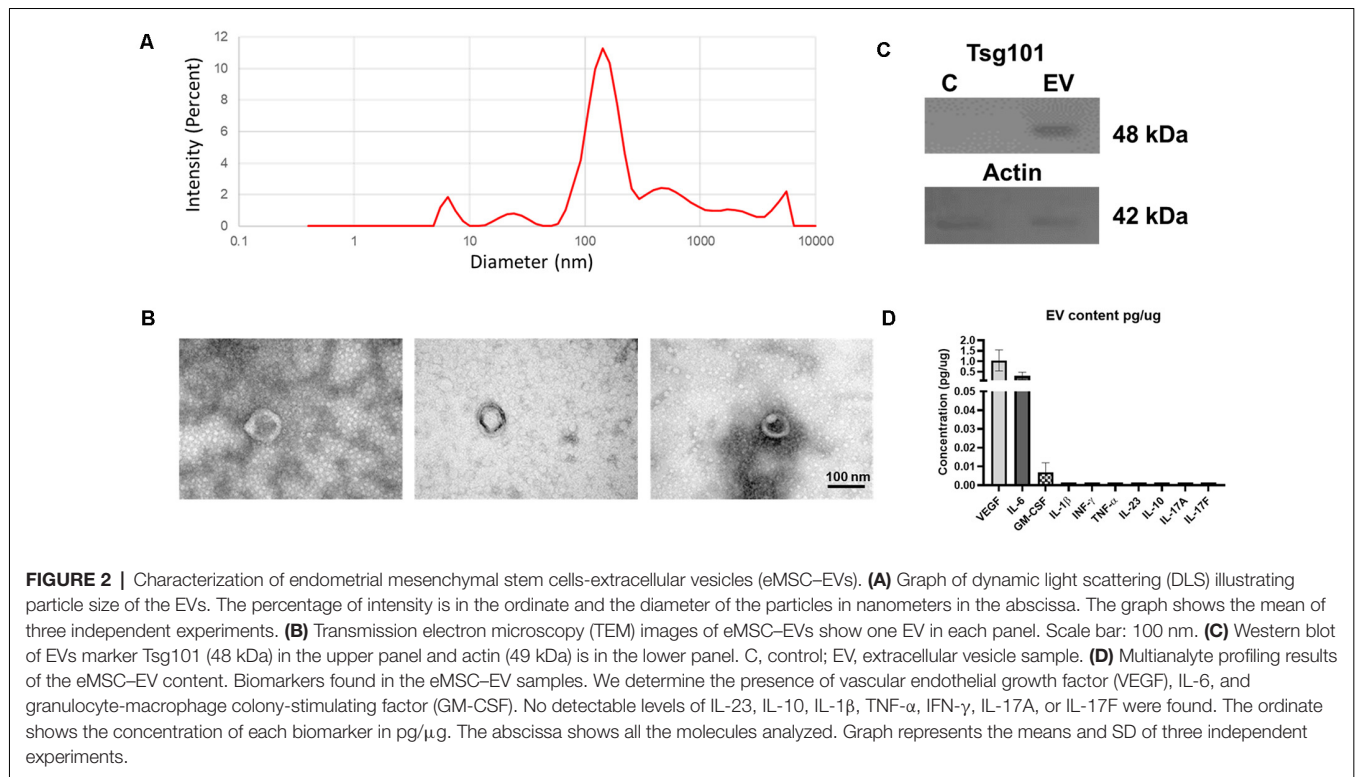
Histological Analysis

At 7 DPI, mice were anesthetized with xylazine/ketamine [intraperitoneal (IP), 80 mg/kg] and intracardially perfused with phosphate-buffered saline (PBS) and fixated with 4% paraformaldehyde in PBS. The brain was immediately removed and postfixed for 48 h at 4°C. The paraffin-embedded area of interest (−1.5 to −2.5 mm from Bregma) was sliced into 5- μ m-thick sections. Approximately 40 slices were obtained and mounted into positively charged slides. We used hematoxylin–eosin staining for assessing the extension of the penetrating brain injury. A representative sample of nine brain

sections was rehydrated in alcohol solutions and then submerged in a 5% hematoxylin solution for 3 min, followed by a 2% eosin solution for 30 s. Slides were finally washed, dehydrated, and sealed with Entellan resin. We observed the brain tissue slices using a light microscope. We examined the ipsilateral and contralateral hemispheres. We measured the depth of the penetrating injury and evaluated the lesion. We observed the neuronal morphological status in the brain tissues of the HI and HIEV groups. The area of the lesion was determined following the brain injury trajectory and considering an area of 0.04 mm² from the center of the lesion. The percentage of pyknotic cells was calculated counting the cells located in the lesion area of CA1, CA2, and DG, in the hippocampus. We used ImageJ software to analyze brain tissue images.

Statistical Analysis

Statistical analyses were carried out in the Minitab 19.2 and GraphPad Prism 8 software. We performed nonparametric Kruskal–Wallis and Wilcoxon tests in behavioral and neurological examinations. For the remaining analyses, multiple *t*-tests and Bonferroni *post hoc* analysis were employed. In all cases, the statistically significant value was taken when $p < 0.05$. We expressed all data as mean \pm SD.



RESULTS

eMSC-EV Characterization

The eMSCs obtained here were adherent to the culture plate and have the characteristic spindle shape. Those cells were positive for CD105, CD73, and CD90 cell markers and negative for hematopoietic CD45 and CD34 markers (data not shown). EVs secreted by these cells were isolated, with a multistep centrifugation and ultrafiltration method. eMSC-EV fractions were characterized according to current standards. DLS of three independent samples showed a peak diameter size at 100–200 nm (Figure 2A). In the sample, we observed round bodies of 100 nm by TEM (Figure 2B). We demonstrated the expression of Tsg101 in eMSC-EVs extracts using Western blot (Figure 2C). MAP results of the eMSC-EVs determined the presence of the growth factors VEGF and GM-CSF at 1.04 ± 0.49 and 0.0072 ± 0.004 pg/ μ g of protein, respectively. IL-6 was also found at 0.30 ± 0.18 pg/ μ g of protein (Figure 2D).

Neurological Outcomes of the Penetrating Hippocampal Injury Model

In hippocampal injury, the neurological score at 3 DPI was 1.8 ± 0.8 . In the cortex lesion, the score was 0.2 ± 0.4 , and the statistical differences were significant with a $p < 0.01$. eMSC-EV administration significantly improved the neurological score to 0.4 ± 0.5 , with statistical significance ($p < 0.05$). At 5 and 7 DPI, the score returned to control value in all groups (Figure 3A).

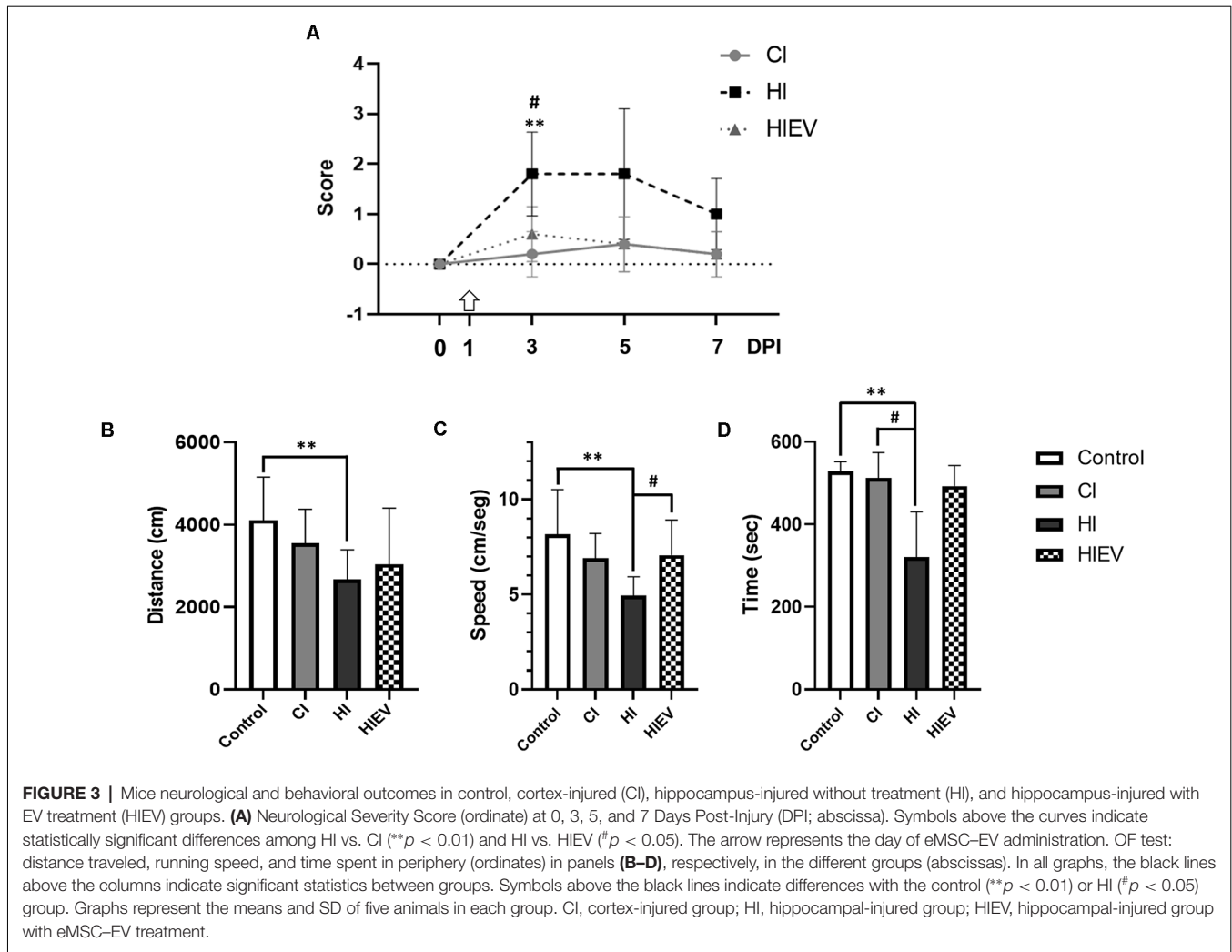
In the OF, we tested mice before the injury (Day 0) as a control group for further comparisons. Figure 3B illustrates that the control group traveled a total distance of $4,113.2 \pm 1,044.1$ cm;

CI, $3,554.0 \pm 823.4$ cm; and HI, $2,671.6 \pm 718.8$ cm. We found statistically significant differences when comparing the HI and control groups ($p < 0.01$). eMSC-EV administration did not improve this parameter. The control group running speed was 8.2 ± 2.3 cm/s. In the cortex and hippocampus injury group, it was 6.9 ± 1.3 and 4.9 ± 0.9 cm/s, respectively. A statistically significant difference was observed between the control and HI groups ($p < 0.01$). eMSC-EV-administered group's running speed was 7.1 ± 1.8 cm/s, statistically significant in comparison with the HI group ($p < 0.05$), see Figure 3C. We evaluated thigmotaxis and fecal boli production in all groups. Control mice spent an average of 528.3 ± 23.2 s in the periphery of the field, similar to what was observed for CI mice (512.9 ± 61.2 s). In HI mice, this behavior decreased to 320.3 ± 110.1 s. Statistically significant differences were detected when compared to the HI vs. control ($p < 0.01$) and HI vs. CI ($p < 0.05$) groups (Figure 3D). The average time in HIEV mice was 492.8 ± 50.2 s, with no statistical differences when compared with the HI group. There were no statistical differences between any groups in fecal boli production.

Locomotion Speed Analysis

We classified mice steps, as stated in *Step Classification*. In control animals, the type of steps with the highest percentage was A. In the HIEV group, Type A steps were predominant. In the CI, the dominant type was B, and in HI were B and C (Figure 4). As Type A was predominant in the control group, we decided to analyze those steps in all groups.

In Type A steps, we found a significant reduction of speed in the right hindlimb of the HI group (23.23 ± 7.13 mm/s) in



comparison with the control group (28.20 ± 7.09 mm/s; $p < 0.01$; **Figure 5A**). Steps speed differences did not occur in the left hindlimb (**Figure 5B**). As differences between all steps were step cycle duration, we decided to analyze the speed considering all types of steps of each mouse.

Considering all steps, in the right hindlimb, control, CI, and HI locomotion speed were 27.72 ± 7.15 , 24.38 ± 7.04 , and 20.66 ± 6.4 mm/s, respectively (**Figure 5C**). We observed statistically significant differences when comparing the control group with the HI ($p < 0.01$) and CI ($p < 0.05$) groups. The speed in the right hindlimb of the HIEV group was 30.53 ± 8.79 mm/s. We found significant differences when compared to the HI vs. HIEV ($p < 0.01$) and HI vs. CI ($p < 0.05$).

In the left hindlimb, the control group speed was 27.87 ± 8.14 ; in the CI group, 29.09 ± 6.05 ; and the HI group speed was 21.94 ± 6.61 mm/s. The differences among the HI vs. control and HI vs. CI groups were statistically significant ($p < 0.01$) in this hindlimb. The decrease in the speed was reversed after the administration of eMSC–EVs: in the HIEV group, the speed was 28.75 ± 6.02 mm/s. No statistical differences occurred when the treated group was compared with control. A significant

difference was found between the HI and HIEV ($p < 0.01$) groups (**Figure 5D**).

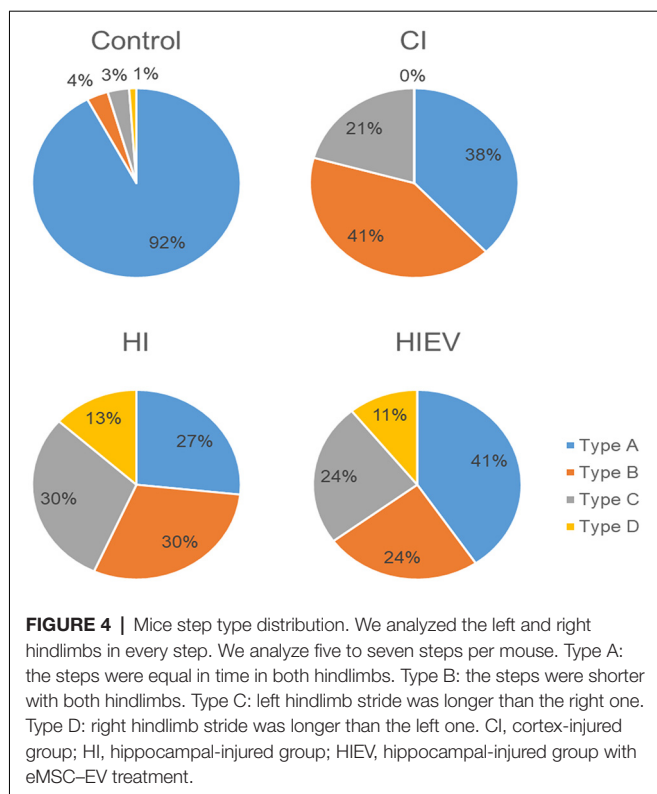
The locomotion speed reduction seen in the HI group could not be attributed to a decrease in the step length, because the step lengths considering all types of steps in all groups did not have differences (data not shown).

Displacement Analysis

We evaluated D_{Min} and D_{Max} of each mouse considering all and Type A steps at 7 DPI. We analyzed D_{Min} values first and considered all steps without classification. We found significance only when comparing the left metatarsus curves of the control vs. HI groups ($p < 0.05$; **Figure 6A**). We did not observe D_{Min} differences between the curves of the groups in the other points of interest.

In respect to D_{Max} values, we found significance when comparing all steps in the curves of the right knee between the HI and HIEV groups ($p < 0.05$), as seen in **Figure 6B**.

We decided to analyze displacement curve differences between Type A steps too, but we did not observe differences when comparing D_{Min} values. We observed improvement of



HIEV groups and differences between the control and HI groups in all points of interest. The right knee comparisons showed statistically significant differences when comparing the control with HI ($p < 0.05$) and HIEV ($p < 0.01$) groups. Significant improvements were observed when EVs were administered and in comparison with the hippocampal injury group ($p < 0.05$), as seen in **Figure 7A**. In the right ankle (**Figure 7B**), we observed differences between the control and HI groups ($p < 0.01$). Also, we found lower D_{Max} values in HI group compared with the HIEV ($p < 0.01$). In **Figure 7C**, lower D_{Max} values were observed in right metatarsus curves of HI groups compared with the control ($p < 0.01$) and HIEV groups ($p < 0.05$).

HI D_{Max} values in left knee were lower when compared with the control ($p < 0.01$), CI ($p < 0.05$), and HIEV ($p < 0.05$) groups (**Figure 8A**). In the left ankle (**Figure 8B**), D_{Max} values showed differences when comparing the control with HI ($p < 0.05$) and HIEV groups ($p < 0.01$). The HI and CI groups also presented statistically significant differences ($p < 0.01$). The left metatarsus D_{Max} graph showed no statistically significant differences between groups (data not shown).

Histological Analysis of the Hippocampus

Cell and tissue loss occurred in the cortex of all groups (**Figure 9**). In the CI group, the hippocampus was not damaged, as shown in **Figure 9A**. In the HI and HIEV groups, the injury reached CA1 and DG. In both hippocampal-damaged groups, the dorsal but not ventral hippocampus was injured. For the histological

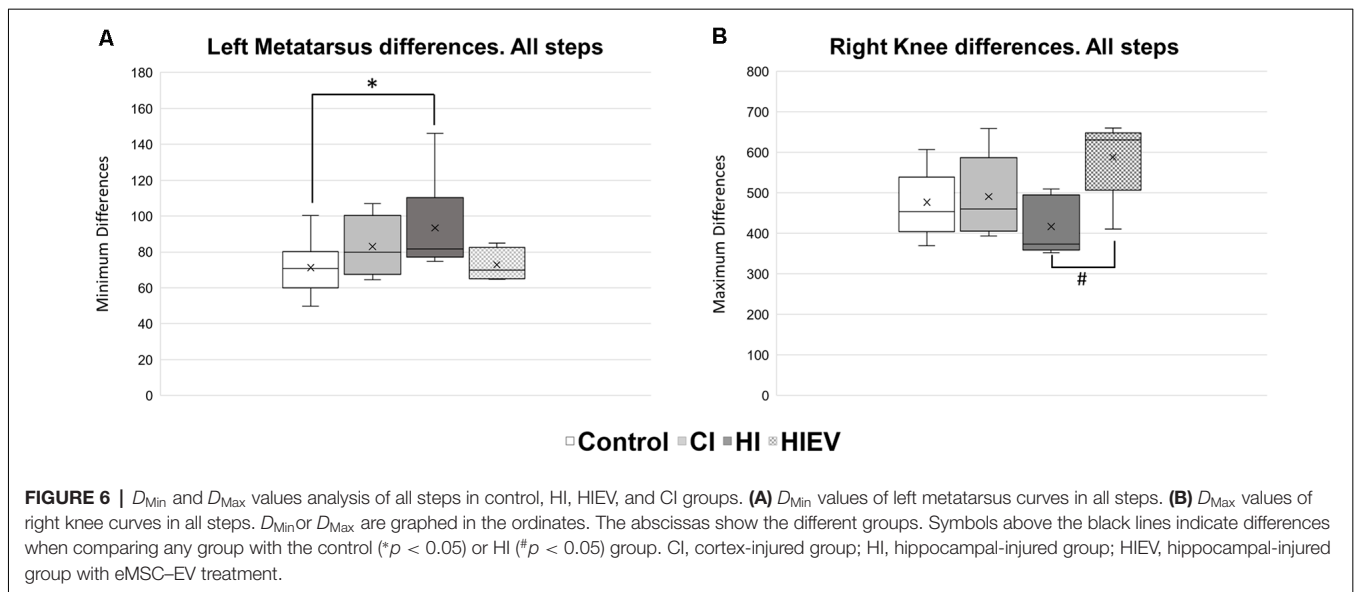
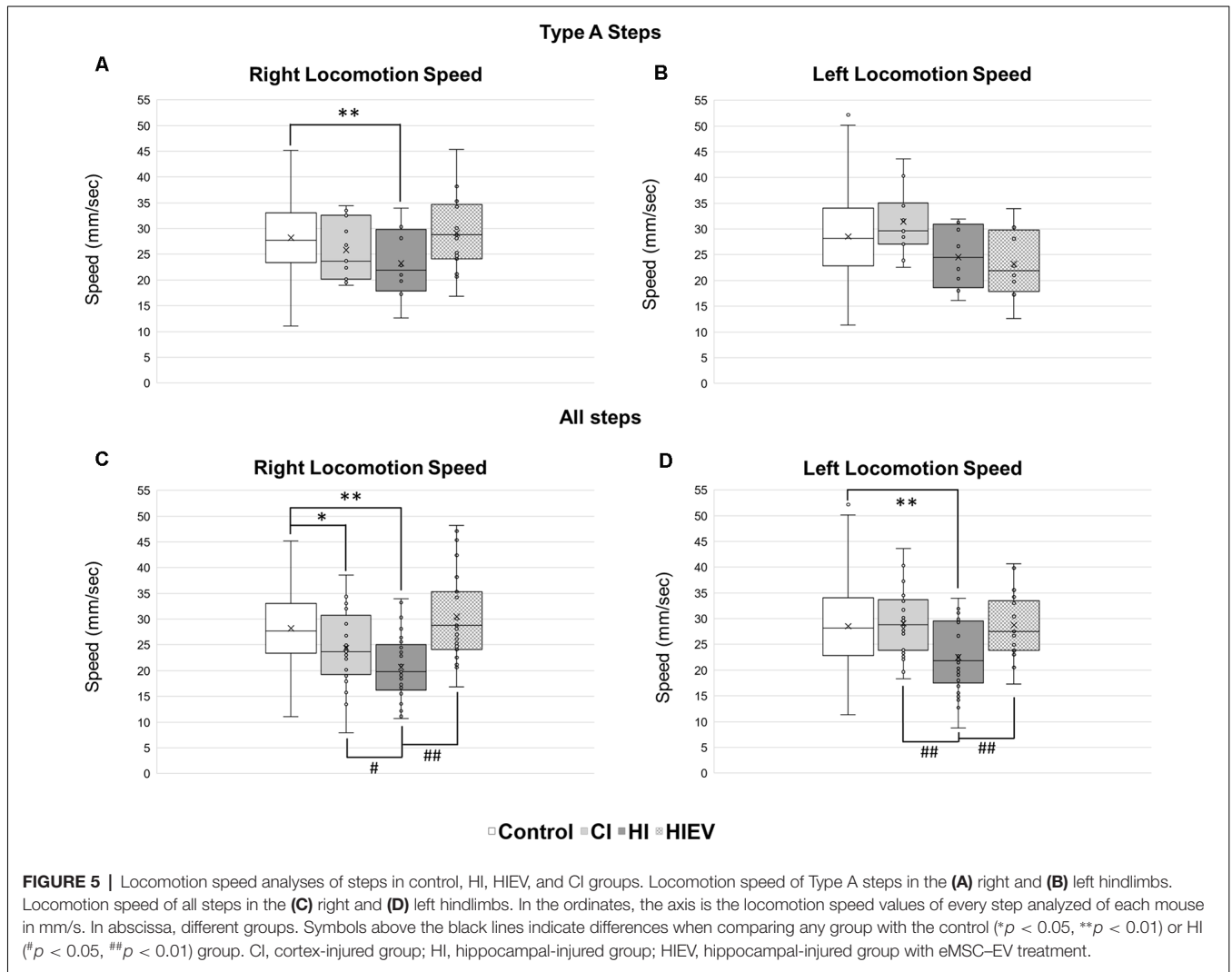
analysis of the hippocampus, we considered only the HI and HIEV groups. Unidentified cells were found in the injury trajectory in the HI and HIEV groups (**Figure 9A**). The percentage of pyknotic cells and injury areas was analyzed and compared. We observed neuronal cell damage in the ipsilateral hemisphere of the HI group. A high percentage of pyknotic cells were found in CA1, CA3, and DG ($61.8\% \pm 8.8\%$, $40\% \pm 8.3\%$, and $68.2\% \pm 7.1\%$, respectively). In HIEV, this damage was more significant in CA1 ($37.2\% \pm 3.9\%$ of pyknotic cells) and DG ($49.2\% \pm 5.9\%$), compared to CA3 ($6.6\% \pm 2.1\%$), see **Figure 9B**. We observed more pyknotic cells in the HI group compared with the HIEV group ($p < 0.01$, **Figure 9C**). In the HI group, the lesion area in the hippocampus was $0.75 \pm 0.09 \text{ mm}^2$. In the HIEV group, it was $0.37 \pm 0.07 \text{ mm}^2$, given a statistically significant difference ($p < 0.01$) between the lesion areas of both groups (**Figure 9D**). Decreases in injury size and neuronal damage were observed after eMSC-EV administration. The contralateral hippocampal hemisphere was undamaged in the three groups (data not shown).

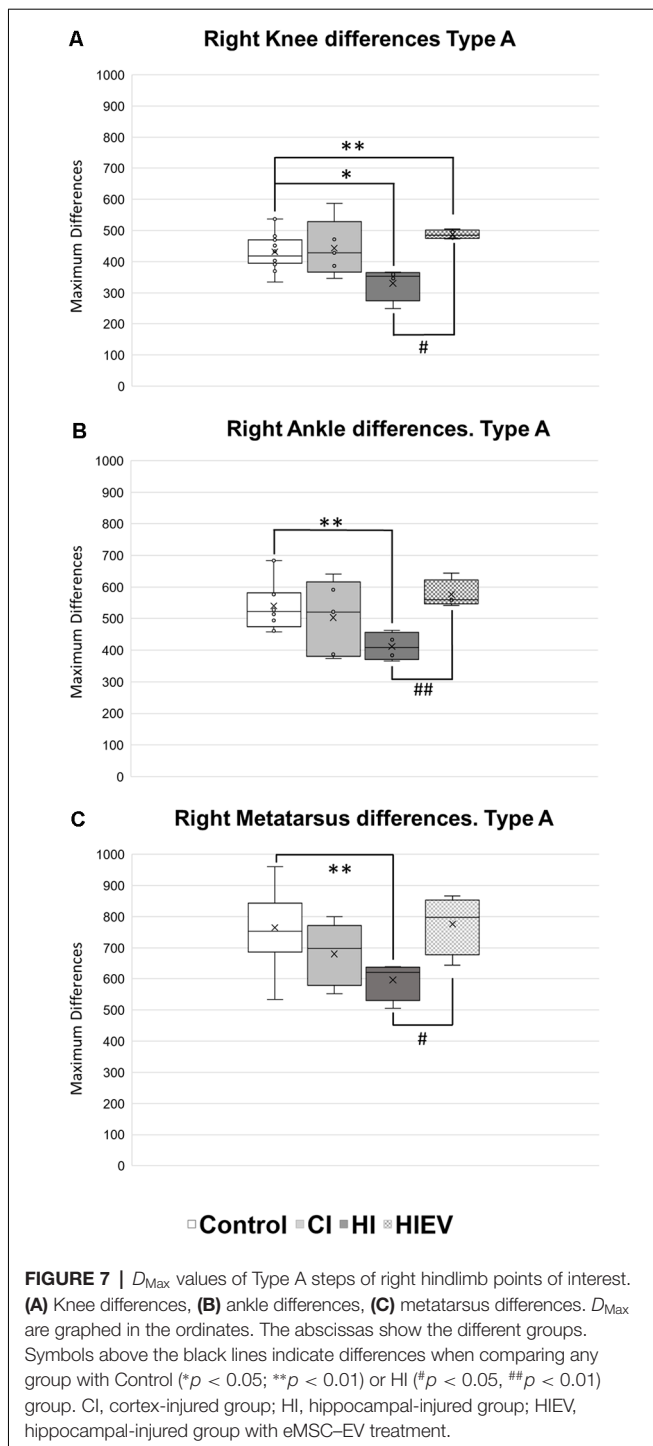
DISCUSSION

To the best of our knowledge, this is the first study to address quantitatively the locomotion speed and displacement in a mouse model of penetrating hippocampal injury, as well as the effect of eMSC-EVs in hippocampal damage through IN administration. We used only male mice because of the preponderance of the bibliography in male animal models. Besides, the estrus cycle in female mice could affect behavior (Xu et al., 2016; Wang et al., 2019), and it is difficult to evaluate the menstrual cycle phases or fluctuating sex hormones for precise comparisons. Stride length, mechanical behaviors, and changes in muscle strength during aging have been described between male and female mice due to sexual hormones (Moran et al., 2005; Bojados et al., 2013; Illien-Jünger et al., 2018). For this, in future studies, it is important to address female and male mice differences in kinematic analyses.

Neuronal apoptosis has been described after TBI in both humans and mice 24–48 h after the injury (Fox et al., 1998; Drefler et al., 2007). In a mouse model of needlestick lesion, a very similar model of ours, gliosis and apoptosis are described 1 day after the damage (Purushothuman et al., 2013). Here, we determined the effect of EVs at 1 DPI. As our model also affects the cortex, we employed a cortical-injured group to analyze the effect of cortex damage alone.

NSS is one of the most used in animal studies. It proves sensorimotor impairments, with motor, equilibrium, and reflex tasks in animals with brain lesions (Schaar et al., 2010; Zarruk et al., 2011). We did not observe sensorimotor impairments in the cortex-injured mice, compared with the control. However, it was noticeable that the HI group had higher scores, compared with all groups. Mice treated with eMSC-EVs after the hippocampal penetrating injury demonstrated reduced sensorimotor deterioration and faster neurological recovery. Despite that we observed recovery in the HI group, this was not completed at 7 DPI. Therefore, spontaneous recovery in eMSC-EV-treated mice can be ruled out.





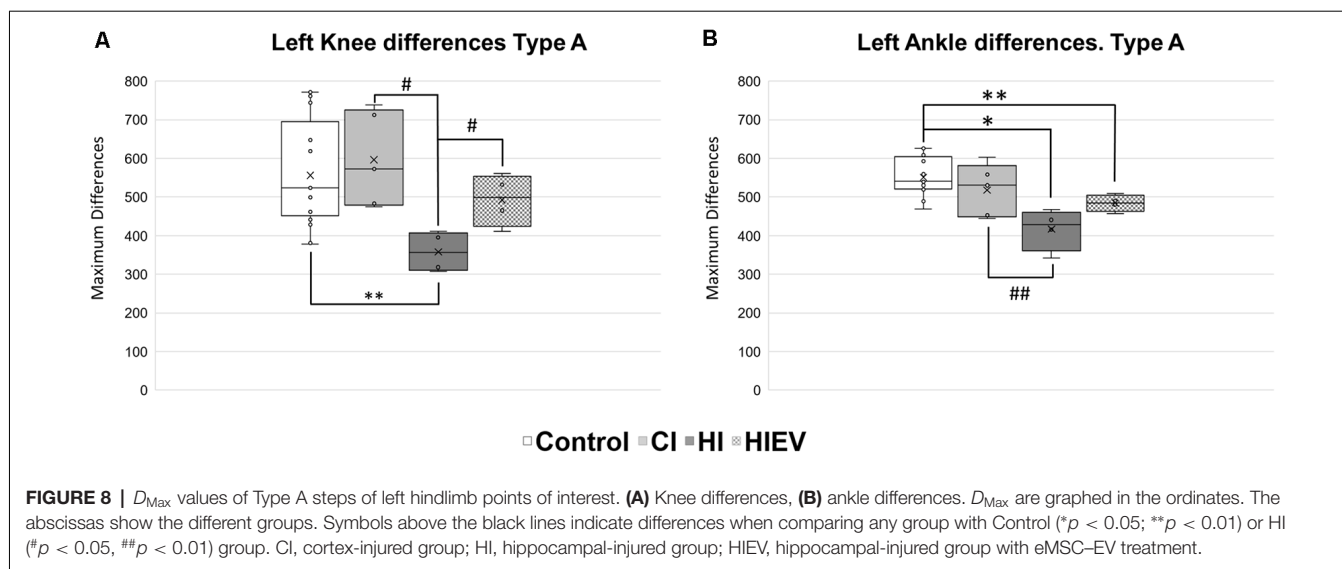
OF test has been extensively used to measure behavior and locomotion, as well as its relationship with hippocampus (Laghmouch et al., 1997). We measured the emotional state in our mice, with thigmotaxis and fecal boli production, as described before, to determine anxiety or fear (Choleris, 2001). We did not find differences in fecal boli production in any groups analyzed. We found a time reduction in the periphery in mice with hippocampus injury compared with the control

group. This could be associated with a diminished anxiety behavior, as it is observed with an anxiolytic drug (Choleris, 2001). There were significant differences between the CI and HI groups in thigmotaxis. This suggests that the behavioral change is mainly due to the hippocampal injury. Similar to what we found, TBI mice with cortex damage did not present any behavioral changes after the injury (Niesman et al., 2014). Moreover, we observed damage only in the dorsal region of the hippocampus. It has been suggested that this region has a main role in spatial memory; meanwhile, ventral region is more involved in sensorial responses and anxiety (Ferbinteanu and McDonald, 2000; Fanselow and Dong, 2010; Bannerman et al., 2014). Despite that any specific hippocampal region has been linked to locomotion, there are several studies in which dorsal hippocampus is modified that associate hippocampus with speed locomotion (Sawińska and Kasicki, 1998; Bender et al., 2015; Hernández-López et al., 2017).

OF test has been used to analyze motor behaviors, mainly locomotor activity. It has been used to study disease models that involve muscular strength or movement capacity impairments (Seibenhener and Wooten, 2015). We found that locomotor activity in all groups was preserved, despite the injuries. However, locomotor speed was reduced in the HI group compared with the control and HIEV groups. The results in behavior and locomotor speed decreased after EV administration suggests that functional recovery could be expected with eMSC-EV IN administration. Behavioral tests, such as OF, provide information about general motor performance and anxiety that could not be separated from each other (Mendes et al., 2015; Rostosky and Milosevic, 2018). To establish the hippocampal role in locomotor control, kinematic analyses are needed (Rostosky and Milosevic, 2018).

We tested the locomotion kinematics of mice using a tunnel walk test. We studied the left and right hindlimbs of every step. In the cortex-injured group, we observed a reduction of step speed only in the right hindlimb when comparing all steps without classification, whereas the injury was made in the left hemisphere. In agreement, the corticospinal tract that originated in the left side in mammals participated in the control of movements in the right side due to the pyramidal decussation at the brainstem level (Vulliamoz et al., 2005; Welniarz et al., 2017). The cortex injury in this work affected primarily sensorimotor areas. However, there is a complex topology of brain networks in the mouse brain (Rubinov et al., 2015). Sensory and motor functions overlap to produce adequate hindlimb movements (Hall and Lindholm, 1974). Also, the connections between S1 and M1 areas are already known (Chakrabarti and Alloway, 2006). For this, motor impairments could be expected in the CI group.

After the CA1 layer was damaged in the HI group, speed reduction was evident in both hindlimbs. In mice, CA1 sensibilization to afferent inputs regulates the running speed (Fuhrmann et al., 2015). Therefore, we can probably presume that, in our studied mice, the speed modulation capacity of the hippocampus was lost. Changes in locomotion speed in a rat model of penetrating hippocampal injury due to CA1 damage were previously described



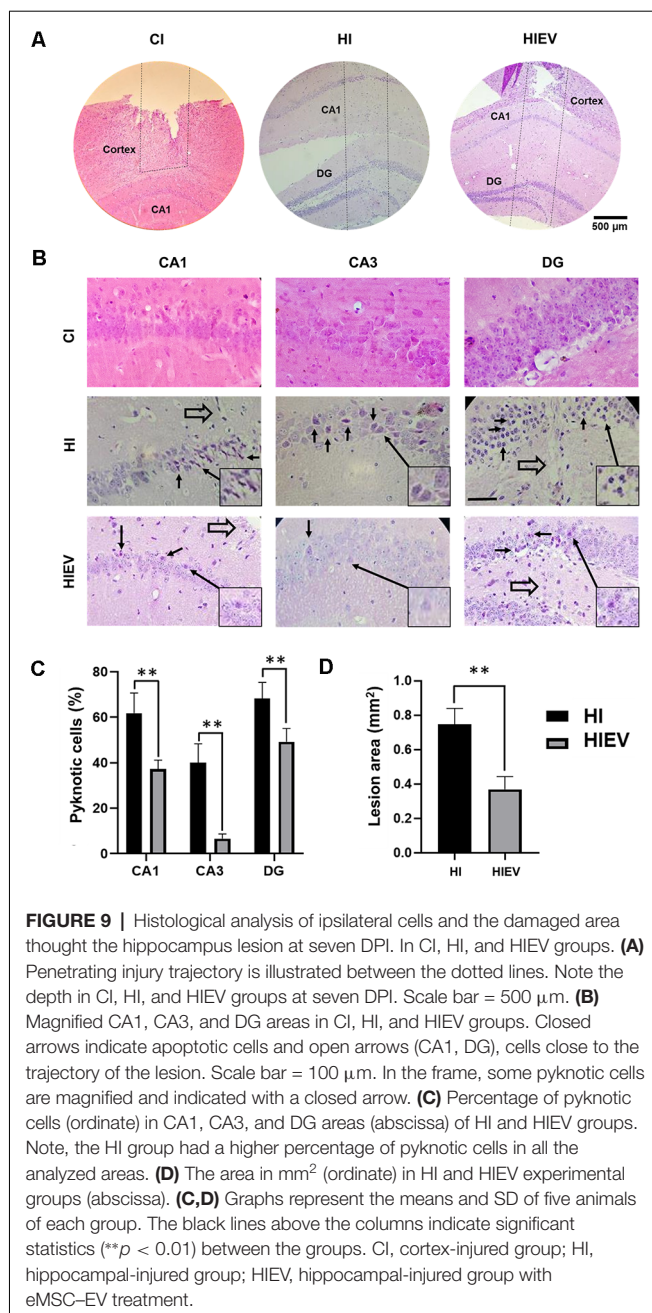
(López Ruiz et al., 2015). Slow walking speed was correlated with functions associated with the hippocampus: impaired processing speed, executive function, and episodic memory (Kim and Won, 2019). Patients with hippocampus pathologies such as Alzheimer disease also experience episodic memory and executive function impairments (Burgess et al., 2002). Hippocampal volume loss is correlated with slower processing speed (Papp et al., 2014; O'Shea et al., 2016) and poorer performance in episodic memory and executive functions (O'Shea et al., 2016). The locomotion speed reduction after hippocampal injury was reversed with eMSC-EV administration. Differences between cortex and hippocampus damage in left hindlimb speed locomotion reveal the different effects of the injured structures.

Increased variability in the type of steps in the cortex-injured group was observed, compared with the control group. Step variability seems to increase when the hippocampus compensates the damage in other brain regions (Beauchet et al., 2019). Our mice presented walk pattern variability, as we observed four different steps. Matching our results, stride abnormalities in individuals with dementia or cognitive impairments included decrease in walking speed (Ijmker and Lamoth, 2012; Doi et al., 2014) and walk variability (Montero-Odasso et al., 2009; Ijmker and Lamoth, 2012; Doi et al., 2014; Beauchet et al., 2019; Zhang et al., 2019). Our findings could be related to clinic symptoms, as hippocampal damage produces walk speed and variability changes in both humans and mice. In elderly people, dual test showed that walking may require more cognitive control than previously thought (Montero-Odasso et al., 2009; Lamoth et al., 2011). In these studies, it was demonstrated that cognitive functions are clearly associated with hippocampal integrity and with speed and step variability (Ijmker and Lamoth, 2012; Doi et al., 2014). There are many characteristics shared between neurodegenerative diseases and the chronic lesion of TBI, including inflammatory and neurovascular pathologies (Purushothuman et al., 2013; Zhou et al., 2020). The lesion described here and the effects

in kinematics could be useful for understanding several human diseases.

We did not observe changes in the displacement curves of the CI group with respect to the control group. We report differences between the displacement curves of HI group only in mice metatarsus when comparing D_{Min} in all steps. In accordance to our findings, metatarsal curve differences were reported in a mouse with hippocampal accumulation of *Toxoplasma* cysts (Galván-Ramírez et al., 2019). Knee D_{Max} differences were evident between the mice with injury and the ones receiving eMSC-EVs. We observed that our method is sensible to step variation, because it did not identify differences with no step classification. When only comparing Type A steps, knee, ankle, and metatarsus displacement curve differences were evident after hippocampal damage in comparison with control group, but only when we compared the most dissimilar curves (D_{Max}). This analysis reveals the variability between group's displacement curves. In all points of interest, the hippocampal-injured mice displacement variability decreases. When hippocampus is damaged, locomotion speed decreases due to alterations of gamma oscillations (Chen et al., 2011). In the HI group, this wave could be altered, and the variation reduction observed could be because these waves are associated with decision making, attention, processing speed, and executive functions and thus the loss of spatial navigation (Ahmed and Mehta, 2012).

We found displacement differences in both hindlimbs in the hippocampal injury group. In rats, the reported changes were only in contralateral hindlimb (López Ruiz et al., 2015). Despite penetrating hippocampal injury was similar in both of our models, there are anatomical and physiological divergences between both rats and mice (Ellenbroek and Youn, 2016). The injury in each species model could affect different pathways that control locomotion in each species and present different results. To address this, a comparative study must be carefully performed.



It has been shown that MSC-EVs can ameliorate impaired hippocampal functions (Deng et al., 2017) and restore synaptic transmission in Schaffer collateral to CA1 synapses (Wang et al., 2018). Hence, the locomotion speed preservation in the eMSC-EV-administered group could be due to CA1 preservation, which in turn could be related to functional recovery, as seen before (López Ruiz et al., 2015). Displacement curves in EV-treated mice returned variability to control values, and in some cases, it became greater. In general, administration of eMSC-EVs improved the outcome of all tests evaluated. In the histology analysis, we observed lower percentage of pyknotic cells and less damaged area in the hippocampus

at 7 DPI after the application of eMSC-EVs in comparison with the nontreated group. This is similar to that reported before in TBI (Li et al., 2017; Ni et al., 2019), stroke (Chen et al., 2016), or Alzheimer disease (Cui et al., 2019; Elia et al., 2019) models.

We identified three factors in eMSC-EVs: VEGF, GM-CSF, and IL-6, in accordance to what is reported for MSC-EVs from different origins (Meng et al., 2007; Alcayaga-Miranda et al., 2015; Lai et al., 2015; Lee et al., 2016). These molecules are related to angiogenesis and neurogenesis and could promote the expression of other neurotrophic factors with neuroprotective effects in the hippocampus (Zhang et al., 2013; Perígolo-vicente et al., 2014; Khan et al., 2015; Sun et al., 2017; Yan et al., 2017; Dougan et al., 2019). Damage prevention of MSC-EVs was observed previously in a TBI rat model, in which the early application reduced the brain inflammatory state and induced cognitive rescue (Kim et al., 2016; Ni et al., 2019). Further studies are needed to determine whether eMSC-EV treatment promotes angiogenesis, neurogenesis, or vascular remodeling, as well as the pathways involved in these mechanisms. In comparison with our study, IN administration of EVs from bone marrow-derived MSCs demonstrated positive effects in the hippocampus (Losurdo et al., 2020).

One limitation of this study is that we did not test the effect of different dosage of eMSC-EVs on hippocampus damage prevention. Future work is required to elucidate the mechanisms of the protective and restorative effects of exosomes and to optimize the dosage and treatment regimen.

CONCLUSION

Penetrating hippocampal injury generates neuron loss in the CA1 region, probably disrupting a network involved in locomotion speed modulation that caused locomotion speed reduction. Displacement changes were also present in mice with hippocampal injury, probably due to loss of spatial navigation. The IN administration of eMSC-EVs after hippocampal injury prevented histological damage and preserved speed locomotion and displacement changes presumably due to the growth factors contained in those vesicles. Our results provide evidence to consolidate the view that the hippocampus plays an essential role in locomotion speed and navigation in rodents and suggest that eMSC-EV IN administration could improve recovery of hippocampal tissue.

DATA AVAILABILITY STATEMENT

The raw data supporting the conclusions of this article will be made available by the authors, without undue reservation.

ETHICS STATEMENT

The animal study was reviewed and approved by “Comité Institucional de Cuidado y Uso de Animales de Laboratorio

(CICUAL),” affiliated to the University of Guadalajara and endorsed to “Comisión Nacional de Bioética” with the number CONBIOÉTICA-14-CEI-002-20191003.

AUTHOR CONTRIBUTIONS

LL-M, RC-A, JR-C, and SD-J contributed to the conception and design of the study. RC-A, JR-C, and SD-J supervised all experiments and data obtention. GM-R and CA-P developed and provided statistical validation to the quantitative kinematics analysis. LL-M, IA-G, and LN-A standardized relevant methods for the experiments of the project. LL-M, ET-A, MD-D, and CG-A contributed to the data obtention, curation, and the formal analysis of the data. LL-M wrote the first draft of the manuscript. RC-A, JD-J, and SD-J revised and edited the manuscript. JR-C obtained financial support for the project.

REFERENCES

- Ahmed, O. J., and Mehta, M. R. (2012). Running speed alters the frequency of hippocampal gamma oscillations. *J. Neurosci.* 32, 7373–7383. doi: 10.1523/JNEUROSCI.5110-11.2012
- Alcayaga-Miranda, F., Cuenca, J., Luz-Crawford, P., Aguila-Díaz, C., Fernandez, A., Figueroa, F. E., et al. (2015). Characterization of menstrual stem cells: angiogenic effect, migration and hematopoietic stem cell support in comparison with bone marrow mesenchymal stem cells. *Stem Cell Res. Ther.* 6:32. doi: 10.1186/s13287-015-0013-5
- Andersen, P., Morris, R., Amaral, D., Bliss, T., and O’Keefe, J. (2007). *The Hippocampus Book*. New York, NY: Oxford University Press.
- Ascencio-Piña, C., Pérez-Cisneros, M., Dueñez-Jimenez, S., and Mendizabal-Ruiz, G. (2020). “A system for high-speed synchronized acquisition of video recording of rodents during locomotion,” in *VIII Latin American Conference on Biomedical Engineering and XLII National Conference on Biomedical Engineering* (Cham: Springer), 309–314.
- Atkins, C. M. (2011). Decoding hippocampal signaling deficits after traumatic brain injury. *Transl. Stroke Res.* 2, 546–555. doi: 10.1007/s12975-011-0123-z
- Bannerman, D. M., Sprengel, R., Sanderson, D. J., Mchugh, S. B., Rawlins, J. N. P., Monyer, H., et al. (2014). Hippocampal synaptic plasticity, spatial memory and anxiety. *Nat. Rev. Neurosci.* 15, 181–192. doi: 10.1038/nrn3677
- Beauchet, O., Launay, C. P., Sekhon, H., Montembeault, M., and Allali, G. (2019). Association of hippocampal volume with gait variability in pre-dementia and dementia stages of Alzheimer disease: results from a cross-sectional study. *Exp. Gerontol.* 115, 55–61. doi: 10.1016/j.exger.2018.11.010
- Bender, F., Gorbati, M., Cadavieco, M. C., Denisova, N., Gao, X., Holman, C., et al. (2015). Theta oscillations regulate the speed of locomotion via a hippocampus to lateral septum pathway. *Nat. Commun.* 6:8521. doi: 10.1038/ncomms9521
- Bland, B. H. (2009). “Anatomical, physiological and pharmacological properties underlying hippocampal sensorimotor integration,” in *Information Processing by Neuronal Populations*, eds C. Holscher and M. Munk (Cambridge, MA: Cambridge University Press), 283–325.
- Bland, B. H., Bland, C. E., and MacIver, M. B. (2016). Median raphe stimulation-induced motor inhibition concurrent with suppression of type 1 and type 2 hippocampal theta. *Hippocampus* 26, 289–300. doi: 10.1002/hipo.22521
- Bojados, M., Herbin, M., and Jamon, M. (2013). Kinematics of treadmill locomotion in mice raised in hypergravity. *Behav. Brain Res.* 244, 48–57. doi: 10.1016/j.bbr.2013.01.017
- Burgess, N., Maguire, E. A., and O’Keefe, J. (2002). The human hippocampus and spatial and episodic memory. *Neuron* 35, 625–641. doi: 10.1016/S0896-6273(02)00830-9
- Cernak, I., Wing, I. D., Davidsson, J., and Plantman, S. (2014). A novel mouse model of penetrating brain injury. *Front. Neurol.* 5:209. doi: 10.3389/fneur.2014.00209

All authors contributed to the article and approved the submitted version.

FUNDING

This work was partially funded by grants from the Consejo Nacional de Ciencia y Tecnología (CONACYT).

ACKNOWLEDGMENTS

We want to thank Luis Enrique Ruiz Herrera for the valuable help in histologic processing, Dalia Alejandra Madrigal Ruiz, for all her support in animal care and welfare and Dr. Suye Suenaga Sánchez and Dr. José Medina Flores, from CryoVida, Banco de Células Madre Humanas for mesenchymal stem cell donation. We thanks Dr. Hugo Guerrero-Cázares for the manuscript revision and his important comments.

- Chakrabarti, S., and Alloway, K. D. (2006). Differential origin of projections from SI barrel cortex to the whisker representations in SII and MI. *J. Comp. Neurol.* 498, 624–636. doi: 10.1002/cne.21052
- Chen, K. H., Chen, C.-H., Wallace, C. G., Yuen, C.-M., Kao, G.-S., Chen, Y.-L., et al. (2016). Intravenous administration of xenogenic adipose-derived mesenchymal stem cells (ADMSC) and ADMSC-derived exosomes markedly reduced brain infarct volume and preserved neurological function in rat after acute ischemic stroke. *Oncotarget* 7, 74537–74556. doi: 10.18632/oncotarget.12902
- Chen, L., Xiang, B., Wang, X., and Xiang, C. (2017). Exosomes derived from human menstrual blood-derived stem cells alleviate fulminant hepatic failure. *Stem Cell Res. Ther.* 8:9. doi: 10.1186/s13287-016-0453-6
- Chen, Z., Resnik, E., McFarland, J. M., Sakmann, B., and Mehta, M. R. (2011). Speed controls the amplitude and timing of the hippocampal gamma rhythm. *PLoS One* 6:e21408. doi: 10.1371/journal.pone.0021408
- Choleris, E. (2001). A detailed ethological analysis of the mouse open field test: effects of diazepam, chlordiazepoxide and an extremely low frequency pulsed magnetic field. *Neurosci. Biobehav. Rev.* 25, 235–260. doi: 10.1016/S0149-7634(01)00011-2
- Cui, G.-H., Guo, H.-D., Li, H., Zhai, Y., Gong, Z.-B., Wu, J., et al. (2019). RVG-modified exosomes derived from mesenchymal stem cells rescue memory deficits by regulating inflammatory responses in a mouse model of Alzheimer’s disease. *Immun. Ageing* 16:10. doi: 10.1186/s12979-019-0150-2
- Dalirfardouei, R., Jamialahmadi, K., Jafarian, A. H., and Mahdipour, E. (2019). Promising effects of exosomes isolated from menstrual blood-derived mesenchymal stem cell on wound-healing process in diabetic mouse model. *J. Tissue Eng. Regen. Med.* 13, 555–568. doi: 10.1002/term.2799
- Deng, M., Xiao, H., Zhang, H., Peng, H., Yuan, H., Xu, Y., et al. (2017). Mesenchymal stem cell-derived extracellular vesicles ameliorates hippocampal synaptic impairment after transient global ischemia. *Front. Cell. Neurosci.* 11:205. doi: 10.3389/fncel.2017.00205
- Doepfner, T. R., Herz, J., Görgens, A., Schlechter, J., Ludwig, A.-K., Radtke, S., et al. (2015). Extracellular vesicles improve post-stroke neuroregeneration and prevent postischemic immunosuppression. *Stem Cells Transl. Med.* 4, 1131–1143. doi: 10.5966/sctm.2015-0078
- Doi, T., Shimada, H., Makizako, H., Tsutsumimoto, K., Uemura, K., Anan, Y., et al. (2014). Cognitive function and gait speed under normal and dual-task walking among older adults with mild cognitive impairment. *BMC Neurol.* 14:67. doi: 10.1186/1471-2377-14-67
- Dougan, M., Dranoff, G., and Dougan, S. K. (2019). GM-CSF, IL-3 and IL-5 family of cytokines: regulators of inflammation. *Immunity* 50, 796–811. doi: 10.1016/j.immuni.2019.03.022
- Drago, D., Cossetti, C., Iraci, N., Gaude, E., Musco, G., Bachi, A., et al. (2013). The stem cell secretome and its role in brain repair. *Biochimie* 95, 2271–2285. doi: 10.1016/j.biochi.2013.06.020

- Drefßler, J., Hanisch, U., Kuhlisch, E., and Geiger, K. D. (2007). Neuronal and glial apoptosis in human traumatic brain injury. *Int. J. Legal Med.* 121, 365–375. doi: 10.1007/s00414-006-0126-6
- Du, X., Yuan, Q., Qu, Y., Zhou, Y., and Bei, J. (2016). Endometrial mesenchymal stem cells isolated from menstrual blood by adherence. *Stem Cells Int.* 2016:3573846. doi: 10.1155/2016/3573846
- Elia, C. A., Tamborini, M., Rasile, M., Desiato, G., Marchetti, S., Swuec, P., et al. (2019). Intracerebral injection of extracellular vesicles from mesenchymal stem cells exerts reduced A β plaque burden in early stages of a preclinical model of Alzheimer's disease. *Cells* 8:1059. doi: 10.3390/cells8091059
- Ellenbroek, B., and Youn, J. (2016). Rodent models in neuroscience research: is it a rat race? *Dis. Model. Mech.* 9, 1079–1087. doi: 10.1242/dmm.026120
- Ezquer, F., Quintanilla, M. E., Morales, P., Santapau, D., Ezquer, M., Kogan, M. J., et al. (2019). Intranasal delivery of mesenchymal stem cell-derived exosomes reduces oxidative stress and markedly inhibits ethanol consumption and post-deprivation relapse drinking. *Addict. Biol.* 24, 994–1007. doi: 10.1111/adb.12675
- Fanselow, M. S., and Dong, H.-W. (2010). Are the dorsal and ventral hippocampus functionally distinct structures? *Neuron* 65, 7–19. doi: 10.1016/j.neuron.2009.11.031
- Ferbinteanu, J., and McDonald, R. J. (2000). Dorsal and ventral hippocampus: same or different? *Psychobiology* 28, 314–324. doi: 10.3758/BF03331990
- Fox, G. B., Fan, L., Levesseur, R. A., and Faden, A. I. (1998). Sustained sensory/motor and cognitive deficits with neuronal apoptosis following controlled cortical impact brain injury in the mouse. *J. Neurotrauma* 15, 599–614. doi: 10.1089/neu.1998.15.599
- Fuhrmann, F., Justus, D., Sosulina, L., Kaneko, H., Beutel, T., Friedrichs, D., et al. (2015). Locomotion, theta oscillations and the speed-correlated firing of hippocampal neurons are controlled by a medial septal glutamatergic circuit. *Neuron* 86, 1253–1264. doi: 10.1016/j.neuron.2015.05.001
- Galván-Ramírez, M. de la L., Salas-Lais, A. G., Dueñas-Jiménez, S. H., Mendizabal-Ruiz, G., Topete, R. F., Berumen-Solis, S. C., et al. (2019). Kinematic locomotion changes in C57BL/6 mice infected with *Toxoplasma* strain ME49. *Microorganisms* 7:573. doi: 10.3390/microorganisms7110573
- Gargett, C. E., Schwab, K. E., Zillwood, R. M., Nguyen, H. P. T., and Wu, D. (2009). Isolation and culture of epithelial progenitors and mesenchymal stem cells from human endometrium. *Biol. Reprod.* 80, 1136–1145. doi: 10.1095/biolreprod.108.075226
- Girgis, F., Pace, J., Sweet, J., and Miller, J. P. (2016). Hippocampal neurophysiologic changes after mild traumatic brain injury and potential neuromodulation treatment approaches. *Front. Syst. Neurosci.* 10:8. doi: 10.3389/fnsys.2016.00008
- Gómez-Virgilio, L., Ramírez-Rodríguez, G. B., Sánchez-Torres, C., Ortiz-López, L., and Meraz-Ríos, M. A. (2018). Soluble factors from human olfactory neural stem/progenitor cells influence the fate decisions of hippocampal neural precursor cells. *Mol. Neurobiol.* 55, 8014–8037. doi: 10.1007/s12035-018-0906-2
- Hall, R. D., and Lindholm, E. P. (1974). Organization of motor and somatosensory neocortex in the albino rat. *Brain Res.* 66, 23–38. doi: 10.1016/0006-8993(74)90076-6
- Hernández-López, F., Rodríguez-Landa, J. F., Puga-Olguín, A., Germán-Ponciano, L. J., Rivadeneyra-Domínguez, E., and Bernal-Morales, B. (2017). Analysis of activity and motor coordination in rats undergoing stereotactic surgery and implantation of a cannula into the dorsal hippocampus. *Neurologia* 32, 579–586. doi: 10.1016/j.nrl.2016.03.004
- Hwang, S.-N., Kim, J.-C., Bhuiyan, M. I. H., Kim, J. Y., Yang, J. S., Yoon, S. H., et al. (2018). Black rice (*Oryza sativa* L., poaceae) extract reduces hippocampal neuronal cell death induced by transient global cerebral ischemia in mice. *Exp. Neurobiol.* 27, 129–138. doi: 10.5607/en.2018.27.2.129
- Ijmker, T., and Lamoth, C. J. C. (2012). Gait and cognition: the relationship between gait stability and variability with executive function in persons with and without dementia. *Gait Posture* 35, 126–130. doi: 10.1016/j.gaitpost.2011.08.022
- Illien-Jünger, S., Palacio-Manchado, P., Kindschuh, W. F., Chen, X., Sroga, G. E., Vashishth, D., et al. (2018). Dietary advanced glycation end products have sex- and age-dependent effects on vertebral bone microstructure and mechanical function in mice. *J. Bone Miner. Res.* 33, 437–448. doi: 10.1002/jbmr.3321
- Jeong, C. H., Kim, S. M., Lim, J. Y., Ryu, C. H., Jun, J. A., and Jeun, S. S. (2014). Mesenchymal stem cells expressing brain-derived neurotrophic factor enhance endogenous neurogenesis in an ischemic stroke model. *Biomed Res. Int.* 2014:129145. doi: 10.1155/2014/129145
- Khan, M., Dhammu, T. S., Matsuda, F., Baarine, M., Dhindsa, T. S., Singh, I., et al. (2015). Promoting endothelial function by S-nitrosoglutathione through the HIF-1 α /VEGF pathway stimulates neurorepair and functional recovery following experimental stroke in rats. *Drug Des. Devel. Ther.* 9, 2233–2247. doi: 10.2147/DDDT.S77115
- Khan, S., Yuldasheva, N. Y., Batten, T. F. C., Pickles, A. R., Kellett, K. A. B., and Saha, S. (2018). Tau pathology and neurochemical changes associated with memory dysfunction in an optimised murine model of global cerebral ischaemia—a potential model for vascular dementia? *Neurochem. Int.* 118, 134–144. doi: 10.1016/j.neuint.2018.04.004
- Kim, D.-K., Nishida, H., An, S. Y., Shetty, A. K., Bartosh, T. J., and Prockop, D. J. (2016). Chromatographically isolated CD63⁺ CD81⁺ extracellular vesicles from mesenchymal stromal cells rescue cognitive impairments after TBI. *Proc. Natl. Acad. Sci. U S A* 113, 170–175. doi: 10.1073/pnas.1522297113
- Kim, M., and Won, C. W. (2019). Sarcopenia is associated with cognitive impairment mainly due to slow gait speed: results from the Korean frailty and aging cohort study (KFACS). *Int. J. Environ. Res. Public Health* 16:1491. doi: 10.3390/ijerph16091491
- Kupcova Skalnikova, H. (2013). Proteomic techniques for characterisation of mesenchymal stem cell secretome. *Biochimie* 95, 2196–2211. doi: 10.1016/j.biochi.2013.07.015
- Laghmouch, A., Bertholet, J. Y., and Crusio, W. E. (1997). Hippocampal morphology and open-field behavior in mus musculus domesticus and Mus spretus inbred mice. *Behav. Genet.* 27, 67–73. doi: 10.1023/A:1025667426222
- Lai, R. C., Yeo, R. W. Y., and Lim, S. K. (2015). Mesenchymal stem cell exosomes. *Semin. Cell Dev. Biol.* 40, 82–88. doi: 10.1016/j.semcdb.2015.03.001
- Lamoth, C. J., Van Deudekom, F. J., Van Campen, J. P., Appels, B. A., De Vries, O. J., and Pijnappels, M. (2011). Gait stability and variability measures show effects of impaired cognition and dual tasking in frail people. *J. Neuroeng. Rehabil.* 8:2. doi: 10.1186/1743-0003-8-2
- Lee, J. Y., Kim, E., Choi, S.-M., Kim, D. W., Kim, K. P., Lee, I., et al. (2016). Microvesicles from brain-extract-treated mesenchymal stem cells improve neurological functions in a rat model of ischemic stroke. *Sci. Rep.* 6:33038. doi: 10.1038/srep33038
- Li, Y., Yang, Y. Y., Ren, J. L., Xu, F., Chen, F.-M., and Li, A. (2017). Exosomes secreted by stem cells from human exfoliated deciduous teeth contribute to functional recovery after traumatic brain injury by shifting microglia M1/M2 polarization in rats. *Stem Cell Res. Ther.* 8:198. doi: 10.1186/s13287-017-0648-5
- Long, Q., Upadhyay, D., Hattiangady, B., Kim, D.-K., An, S. Y., Shuai, B., et al. (2017). Intranasal MSC-derived A1-exosomes ease inflammation and prevent abnormal neurogenesis and memory dysfunction after status epilepticus. *Proc. Natl. Acad. Sci. U S A* 114, E3536–E3545. doi: 10.1073/pnas.1703920114
- López Ruiz, J. R., Osuna Carrasco, L. P., López Valenzuela, C. L., Franco Rodríguez, N. E., de la Torre Valdovinos, B., Jiménez Estrada, L., et al. (2015). The hippocampus participates in the control of locomotion speed. *Neuroscience* 311, 207–215. doi: 10.1016/j.neuroscience.2015.10.034
- Losurdo, M., Pedrazzoli, M., D'Agostino, C., Elia, C. A., Massenzio, F., Lonati, E., et al. (2020). Intranasal delivery of mesenchymal stem cell-derived extracellular vesicles exerts immunomodulatory and neuroprotective effects in a 3xTg model of Alzheimer's disease. *Stem Cells Transl. Med.* 9, 1068–1084. doi: 10.1002/sctm.19-0327
- Lötvall, J., Hill, A. F., Hochberg, F., Buzás, E. I., Vizio, D. D., Gardiner, C., et al. (2014). Minimal experimental requirements for definition of extracellular vesicles and their functions: a position statement from the international society for extracellular vesicles. *J. Extracell. Vesicles* 3:26913. doi: 10.3402/jev.v3.26913
- Lu, L., Ren, Y., Yu, T., Liu, Z., Wang, S., Tan, L., et al. (2020). Control of locomotor speed, arousal and hippocampal theta rhythms by the nucleus incertus. *Nat. Commun.* 11:262. doi: 10.1038/s41467-019-14116-y
- Mahdipour, E., Salmasi, Z., and Sabeti, N. (2019). Potential of stem cell-derived exosomes to regenerate β islets through Pdx-1 dependent mechanism in a rat

- model of type 1 diabetes. *J. Cell. Physiol.* 234, 20310–20321. doi: 10.1002/jcp.28631
- Mendes, C. S., Bartos, I., Márka, Z., Akay, T., Márka, S., and Mann, R. S. (2015). Quantification of gait parameters in freely walking rodents. *BMC Biol.* 13:50. doi: 10.1186/s12915-015-0154-0
- Meng, X., Ichim, T. E., Zhong, J., Rogers, A., Yin, Z., Jackson, J., et al. (2007). Endometrial regenerative cells: a novel stem cell population. *J. Transl. Med.* 5:57. doi: 10.1186/1479-5876-5-57
- Montero-Odasso, M., Casas, A., Hansen, K. T., Bilski, P., Gutmanis, I., Wells, J. L., et al. (2009). Quantitative gait analysis under dual-task in older people with mild cognitive impairment: a reliability study. *J. Neuroeng. Rehabil.* 6:35. doi: 10.1186/1743-0003-6-35
- Moran, A. L., Warren, G. L., and Lowe, D. A. (2005). Soleus and EDL muscle contractility across the lifespan of female C57BL/6 mice. *Exp. Gerontol.* 40, 966–975. doi: 10.1016/j.exger.2005.09.005
- Musina, R. A., Belyavski, A. V., Tarusova, O. V., Solovyova, E. V., and Sukhikh, G. T. (2008). Endometrial mesenchymal stem cells isolated from the menstrual blood. *Bull. Exp. Biol. Med.* 145, 539–543. doi: 10.1007/s10517-008-0136-0
- Ni, H., Yang, S., Siaw-Debrah, F., Hu, J., Wu, K., He, Z., et al. (2019). Exosomes derived from bone mesenchymal stem cells ameliorate early inflammatory responses following traumatic brain injury. *Front. Neurosci.* 13:14. doi: 10.3389/fnins.2019.00014
- Niesman, I. R., Schilling, J. M., Shapiro, L. A., Kellerhals, S. E., Bonds, J. A., Kleschevnikov, A. M., et al. (2014). Traumatic brain injury enhances neuroinflammation and lesion volume in caveolin deficient mice. *J. Neuroinflammation* 11:39. doi: 10.1186/1742-2094-11-39
- Nikonenko, A. G., Radenovic, L., Andjus, P. R., and Skibo, G. G. (2009). Structural features of ischemic damage in the hippocampus. *Anat. Rec.* 292, 1914–1921. doi: 10.1002/ar.20969
- O'Shea, A., Cohen, R. A., Porges, E. C., Nissim, N. R., and Woods, A. J. (2016). Cognitive aging and the hippocampus in older adults. *Front. Aging Neurosci.* 8:298. doi: 10.3389/fnagi.2016.00298
- Pachler, K., Lener, T., Streif, D., Dunai, Z. A., Desgeorges, A., Feichtner, M., et al. (2017). A good manufacturing practice-grade standard protocol for exclusively human mesenchymal stromal cell-derived extracellular vesicles. *Cytotherapy* 19, 458–472. doi: 10.1016/j.jcyt.2017.01.001
- Papp, K. V., Kaplan, R. F., Springate, B., Moscufo, N., Wakefield, D. B., Guttman, C. R. G., et al. (2014). Processing speed in normal aging: effects of white matter hyperintensities and hippocampal volume loss. *Neuropsychol. Dev. Cogn. B Aging Neuropsychol. Cogn.* 21, 197–213. doi: 10.1080/13825585.2013.795513
- Paquet, J., Deschepper, M., Moya, A., Logeart-Avramoglou, D., Boisson-Vidal, C., and Petite, H. (2015). Oxygen tension regulates human mesenchymal stem cell paracrine functions. *Stem Cells Transl. Med.* 4, 809–821. doi: 10.5966/sctm.2014-0180
- Perigolo-vicente, R., Ritt, K., Gonçalves-de-albuquerque, C. F., Castro-fariante, H. C., Paes-de-carvalho, R., and Giestal-de-araujo, E. (2014). IL-6, A1 and A2aR: a crosstalk that modulates BDNF and induces neuroprotection. *Biochem. Biophys. Res. Commun.* 449, 477–482. doi: 10.1016/j.bbrc.2014.05.036
- Purushothuman, S., Marotte, L., Stowe, S., Johnstone, D. M., and Stone, J. (2013). The response of cerebral cortex to haemorrhagic damage: experimental evidence from a penetrating injury model. *PLoS One* 8:e59740. doi: 10.1371/journal.pone.0059740
- Rostovsky, C. M., and Milosevic, I. (2018). Gait analysis of age-dependent motor impairments in mice with neurodegeneration. *J. Vis. Exp.* 136:e57752. doi: 10.3791/57752
- Rubinov, M., Ypma, R. J. F., Watson, C., Bullmore, E. T., and Raichle, M. E. (2015). Wiring cost and topological participation of the mouse brain connectome. *Proc. Natl. Acad. Sci. U S A* 112, 10032–10037. doi: 10.1073/pnas.1420315112
- Saribas, G. S., Ozogul, C., Tiryaki, M., Alpaslan Pinarli, F., and Hamdemir Kilic, S. (2019). Effects of uterus derived mesenchymal stem cells and their exosomes on asherman's syndrome. *Acta Histochem.* 122:151465. doi: 10.1016/j.acthis.2019.151465
- Seibenhener, M. L., and Wooten, M. C. (2015). Use of the open field maze to measure locomotor and anxiety-like behavior in mice. *J. Vis. Exp.* 96:e52434. doi: 10.3791/52434
- Schaar, K. L., Brenneman, M. M., and Savitz, S. I. (2010). Functional assessments in the rodent stroke model. *Exp. Transl. Stroke Med.* 2:13. doi: 10.1186/2040-7378-2-13
- Shively, S., Scher, A. I., Perl, D. P., and Diaz-Arrastia, R. (2012). Dementia resulting from traumatic brain injury: what is the pathology? *Arch. Neurol.* 69, 1245–1251. doi: 10.1001/archneurol.2011.3747
- Singh, V., Krishan, P., and Shri, R. (2018). Antioxidant-mediated neuroprotection by *Allium schoenoprasum* L. leaf extract against ischemia reperfusion-induced cerebral injury in mice. *J. Basic Clin. Physiol. Pharmacol.* 29, 403–410. doi: 10.1515/jbcp-2017-0070
- Sawińska, U., and Kasicki, S. (1998). The frequency of rat's hippocampal theta rhythm is related to the speed of locomotion. *Brain Res.* 796, 327–331. doi: 10.1016/S0006-8993(98)00390-4
- Sun, L., Li, Y., Jia, X., Wang, Q., Li, Y., Hu, M., et al. (2017). Neuroprotection by IFN- γ via astrocyte-secreted IL-6 in acute neuroinflammation. *Oncotarget* 8, 40065–40078. doi: 10.18632/oncotarget.16990
- Tucker, L. B., Burke, J. F., Fu, A. H., and McCabe, J. T. (2017). Neuropsychiatric symptom modeling in male and female C57BL/6J mice after experimental traumatic brain injury. *J. Neurotrauma* 34, 890–905. doi: 10.1089/neu.2016.4508
- Vulliamoz, S., Raineteau, O., and Jabaudon, D. (2005). Reaching beyond the midline: why are human brains cross wired? *Lancet Neurol.* 4, 87–99. doi: 10.1016/S1474-4422(05)00990-7
- Wang, C., Zhang, Y., Shao, S., Cui, S., Wan, Y., and Yi, M. (2019). Ventral hippocampus modulates anxiety-like behavior in male but not female C57BL/6 J mice. *Neuroscience* 418, 50–58. doi: 10.1016/j.neuroscience.2019.08.032
- Wang, K., Jiang, Z., Webster, K. A., Chen, J., Hu, H., Zhou, Y., et al. (2017). Enhanced cardioprotection by human endometrium mesenchymal stem cells driven by exosomal microRNA-21. *Stem Cells Transl. Med.* 6, 209–222. doi: 10.5966/sctm.2015-0386
- Wang, S.-S., Jia, J., and Wang, Z. (2018). Mesenchymal stem cell-derived extracellular vesicles suppresses iNOS expression and ameliorates neural impairment in Alzheimer's disease mice. *J. Alzheimer's Dis.* 61, 1005–1013. doi: 10.3233/JAD-170848
- Welniarz, Q., Dusart, I., and Roze, E. (2017). The corticospinal tract: evolution, development and human disorders. *Dev. Neurobiol.* 77, 810–829. doi: 10.1002/dneu.22455
- Williams, A. M., Dennahy, I. S., Bhatti, U. F., Halaweish, I., Xiong, Y., Chang, P., et al. (2019). Mesenchymal stem cell-derived exosomes provide neuroprotection and improve long-term neurologic outcomes in a swine model of traumatic brain injury and hemorrhagic shock. *J. Neurotrauma* 36, 54–60. doi: 10.1089/neu.2018.5711
- Xin, H., Li, Y., Cui, Y., Yang, J. J., Zhang, Z. G., and Chopp, M. (2013). Systemic administration of exosomes released from mesenchymal stromal cells promote functional recovery and neurovascular plasticity after stroke in rats. *J. Cereb. Blood Flow Metab.* 33, 1711–1715. doi: 10.1038/jcbfm.2013.152
- Xu, Y., Sheng, H., Bao, Q., Wang, Y., Lu, J., and Ni, X. (2016). NLRP3 inflammasome activation mediates estrogen deficiency-induced depression- and anxiety-like behavior and hippocampal inflammation in mice. *Brain Behav. Immun.* 56, 175–186. doi: 10.1016/j.bbi.2016.02.022
- Yan, H., Feng, Y., and Wang, Q. (2016). Altered effective connectivity of hippocampus-dependent episodic memory network in mTBI survivors. *Neural Plast.* 2016:6353845. doi: 10.1155/2016/6353845
- Yan, M., Hu, Y., Yao, M., Bao, S., and Fang, Y. (2017). GM-CSF ameliorates microvascular barrier integrity via pericyte-derived Ang-1 in wound healing. *Wound Repair Regen.* 25, 933–943. doi: 10.1111/wrr.12608
- Zarruk, J. G., Garcia-Yebenes, I., Romera, V. G., Ballesteros, I., Moraga, A., Cuartero, M. I., et al. (2011). Neurological tests for functional outcome assessment in rodent models of ischaemic stroke. *Rev. Neurol.* 53, 607–618. doi: 10.33588/rn.5310.2011016
- Zhang, R. L., Zhang, Z. G., and Chopp, M. (2013). Targeting nitric oxide in the subacute restorative treatment of ischemic stroke. *Expert Opin. Investig. Drugs* 22, 843–851. doi: 10.1517/13543784.2013.793672

- Zhang, W., Low, L. F., Gwynn, J. D., and Clemson, L. (2019). Interventions to improve gait in older adults with cognitive impairment: a systematic review. *J. Am. Geriatr. Soc.* 67, 381–391. doi: 10.1111/jgs.15660
- Zhang, Y., Chopp, M., Meng, Y., Katakowski, M., Xin, H., Mahmood, A., et al. (2015). Effect of exosomes derived from multipotent mesenchymal stromal cells on functional recovery and neurovascular plasticity in rats after traumatic brain injury. *J. Neurosurg.* 122, 856–867. doi: 10.3171/2014.11.JNS14770
- Zhang, Y., Chopp, M., Zhang, Z. G., Katakowski, M., Xin, H., Qu, C., et al. (2017). Systemic administration of cell-free exosomes generated by human bone marrow derived mesenchymal stem cells cultured under 2D and 3D conditions improves functional recovery in rats after traumatic brain injury. *Neurochem. Int.* 111, 69–81. doi: 10.1016/j.neuint.2016.08.003
- Zhou, Y., Chen, Q., Wang, Y., Wu, H., Xu, W., Pan, Y., et al. (2020). Persistent neurovascular unit dysfunction: pathophysiological substrate and trigger for late-onset neurodegeneration after traumatic brain injury. *Front. Neurosci.* 14:581. doi: 10.3389/fnins.2020.00581
- Conflict of Interest:** The authors declare that the research was conducted in the absence of any commercial or financial relationships that could be construed as a potential conflict of interest.
- Copyright © 2020 León-Moreno, Castañeda-Arellano, Aguilar-García, Desentis-Desentis, Torres-Anguiano, Gutiérrez-Almeida, Najjar-Acosta, Mendizabal-Ruiz, Ascencio-Piña, Dueñas-Jiménez, Rivas-Carrillo and Dueñas-Jiménez. This is an open-access article distributed under the terms of the Creative Commons Attribution License (CC BY). The use, distribution or reproduction in other forums is permitted, provided the original author(s) and the copyright owner(s) are credited and that the original publication in this journal is cited, in accordance with accepted academic practice. No use, distribution or reproduction is permitted which does not comply with these terms.